Electronic Supplementary Material (ESI) for Journal of Materials Chemistry A. This journal is © The Royal Society of Chemistry 2021

Supporting Information for

Pt-on-Pd bimetallic nanodendrites stereoassembled on MXene nanosheets for use as high-efficiency electrocatalysts toward the methanol oxidation reaction

Cuizhen Yang[a], Quanguo Jiang[a], Huan Liu[a], Lu Yang[a], Haiyan He[a], Huajie Huang[a], and Weihua Li[b]**

[a]College of Mechanics and Materials, Hohai University, Nanjing 210098, China
[b]College of Chemical Engineering and Technology, Sun Yat-sen University, Tangjiawan, Zhuhai, 519082, China

E-mail: huanghuajie@hhu.edu.cn or liweihua3@mail.sysu.edu.cn

Supplementary Results

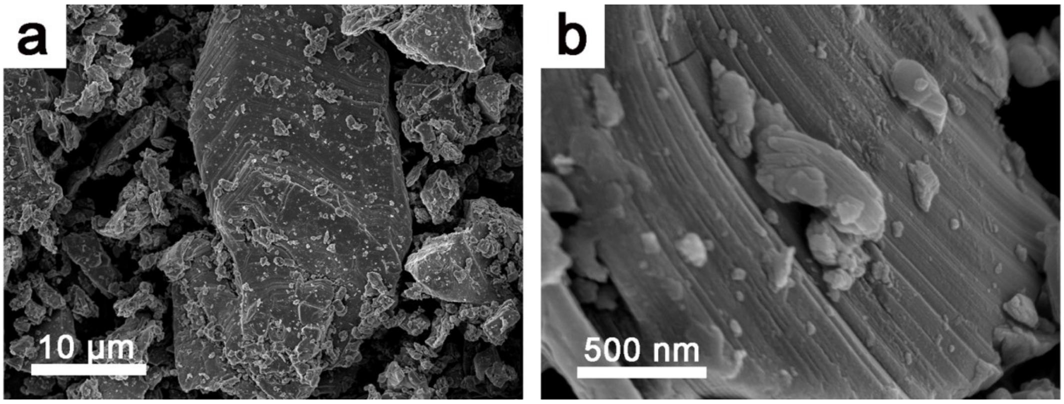

Fig. S1 Representative SEM images of the bulk Ti_3AlC_2 powder.

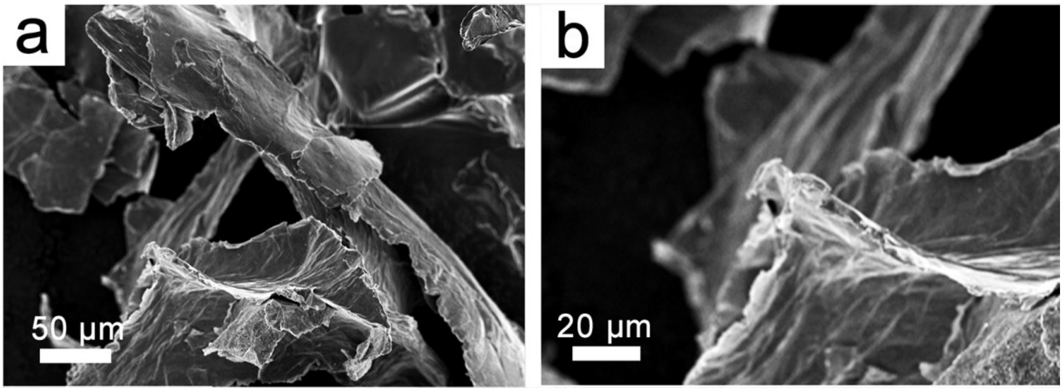

Fig. S2 Representative SEM images of the exfoliated $Ti_3C_2T_x$ nanosheets.

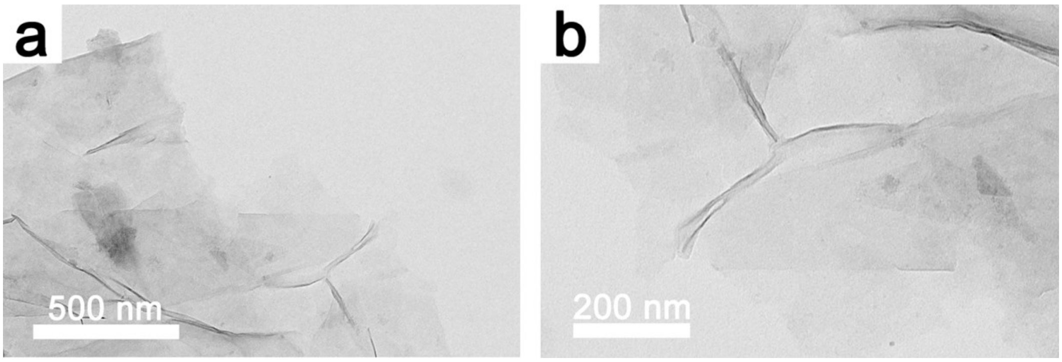

Fig. S3 Representative TEM images of the exfoliated $Ti_3C_2T_x$ nanosheets.

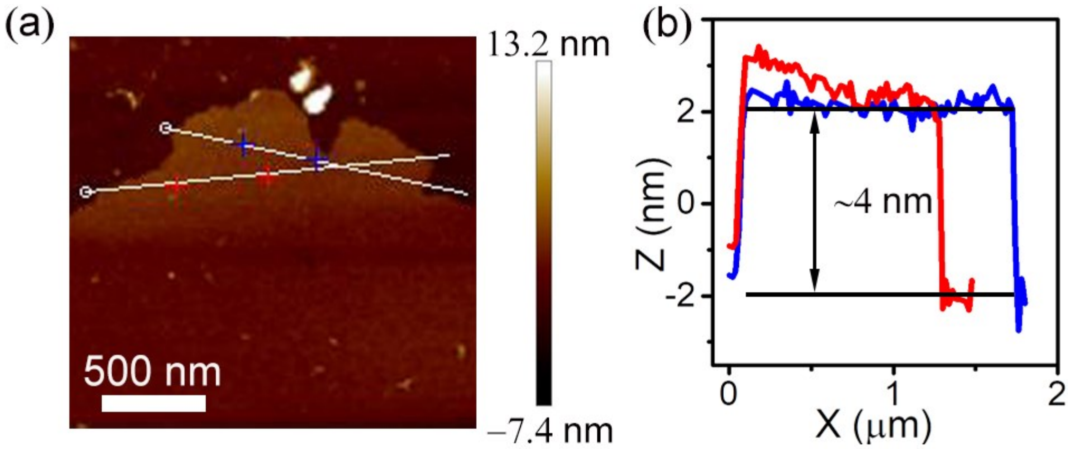

Fig. S4 (a) AFM image of the exfoliated $Ti_3C_2T_x$ nanosheets and (b) the corresponding thickness analysis along the white lines in (a) discloses that the uniform thickness of the $Ti_3C_2T_x$ nanosheets is about 4.0 nm.

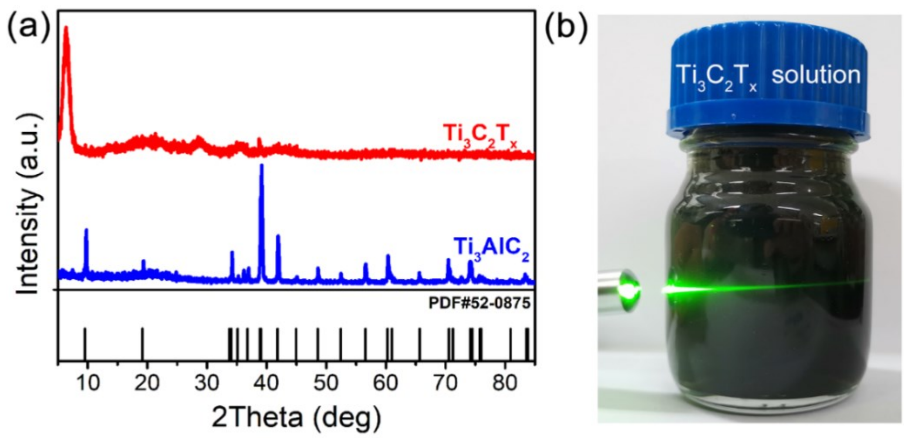

Fig. S5 (a) The XRD patterns of the Ti_3AlC_2 powder and $Ti_3C_2T_x$ nanosheets; (b) The digital photographs of $Ti_3C_2T_x$ solution showing the Tyndall scattering effect.

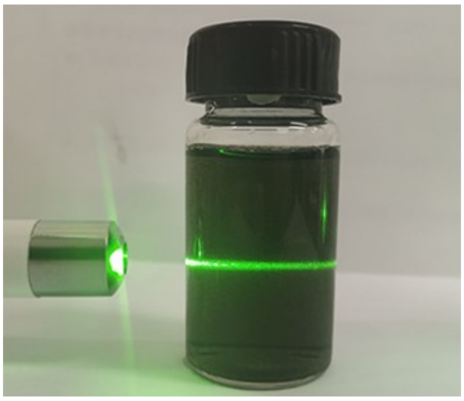

Fig. S6 The Tyndall effect confirming the colloidal nature of the PVP-functionalized $Ti_3C_2T_x$ solution.

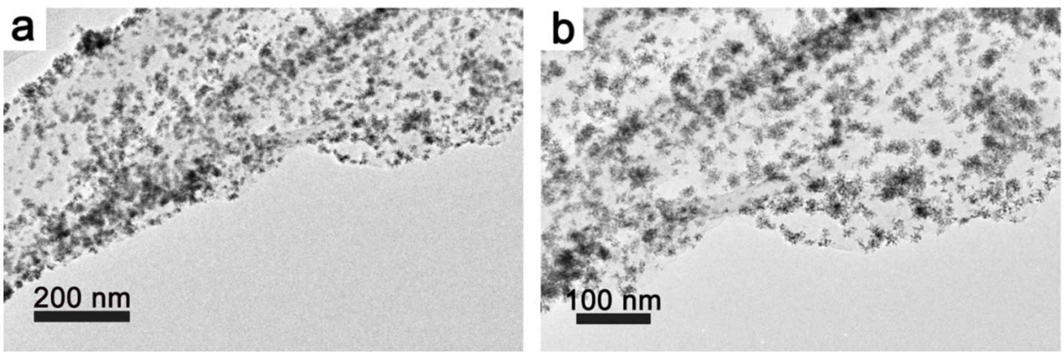

Fig. S7 TEM images of the Pt-on-Pd/$Ti_3C_2T_x$ hybrid with different magnifications, implying a uniform distribution of Pt-on-Pd nanoflowers on the $Ti_3C_2T_x$ nanosheets.

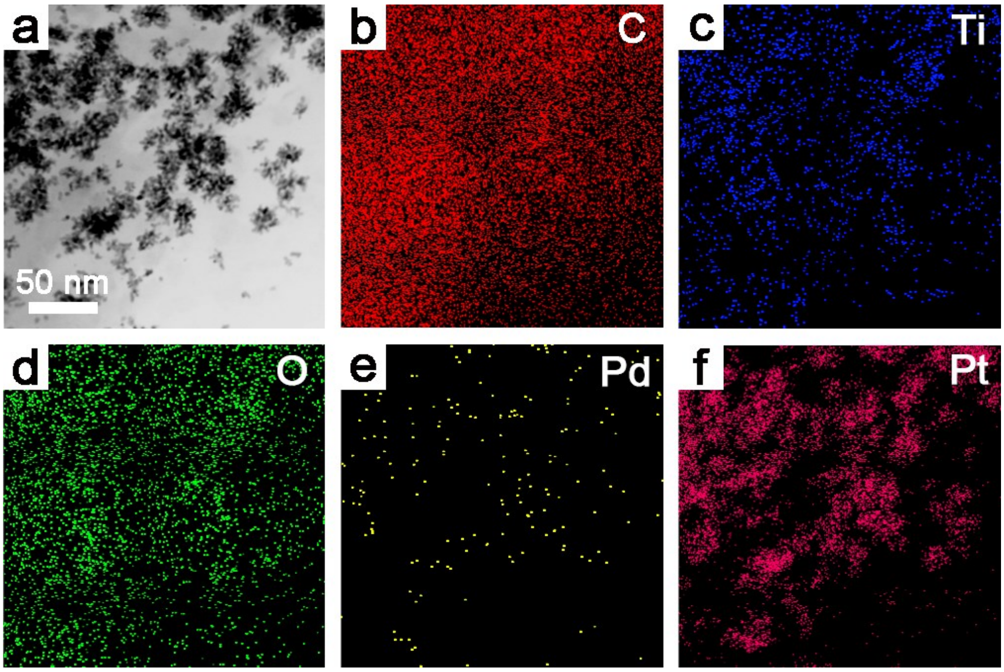

Fig. S8 (a) TEM image of the Pt-on-Pd/$Ti_3C_2T_x$ hybrid and the corresponding elemental mapping images of (b) C, (c) Ti, (d) O, (e) Pd and (f) Pt elements.

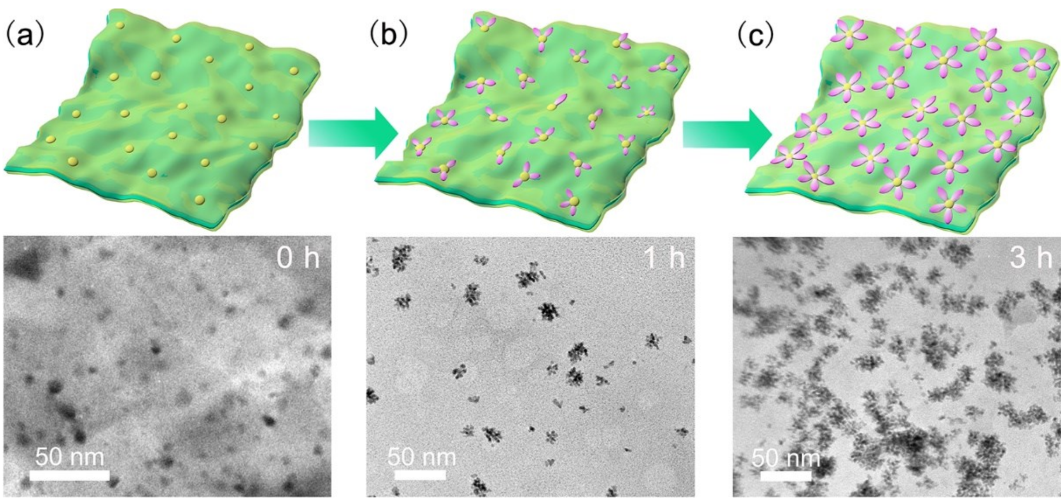

Fig. S9 TEM images of intermediate products extracted from the reaction mixture of Pt-on-Pd bimetallic nanodendrite/$Ti_3C_2T_x$ hybrids at different reaction times：(a) 0 h; (b)1 h; (c) 3 h.

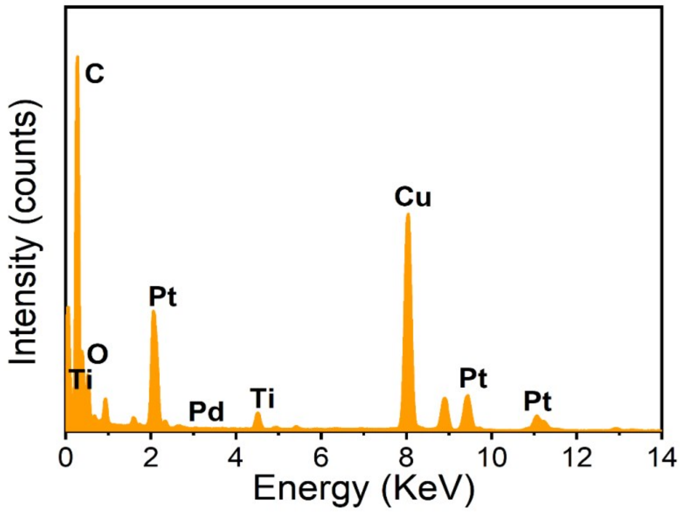

Fig. S10 EDX spectrum of the Pt-on-Pd/$Ti_3C_2T_x$ samples confirms the co-existence of C, O, Ti, Pd and Pt components in the material. The Cu peaks were also observable because the sample was held on a Cu grid.

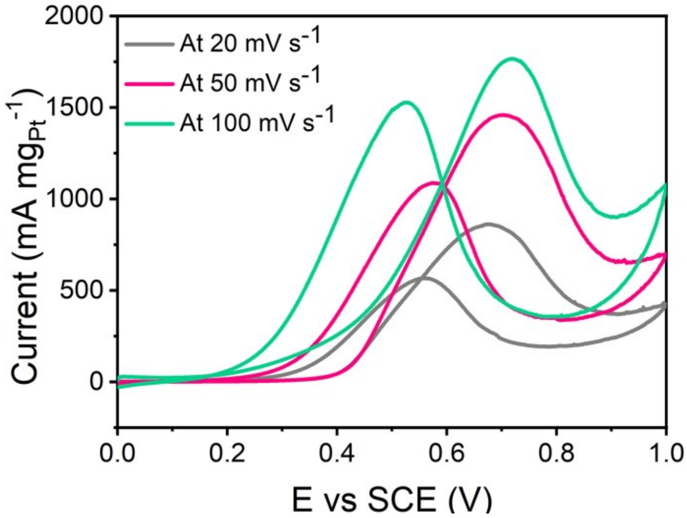

Fig. S11 The CV curves of the Pt-on-Pd/$Ti_3C_2T_x$ catalyst with different scan rates.

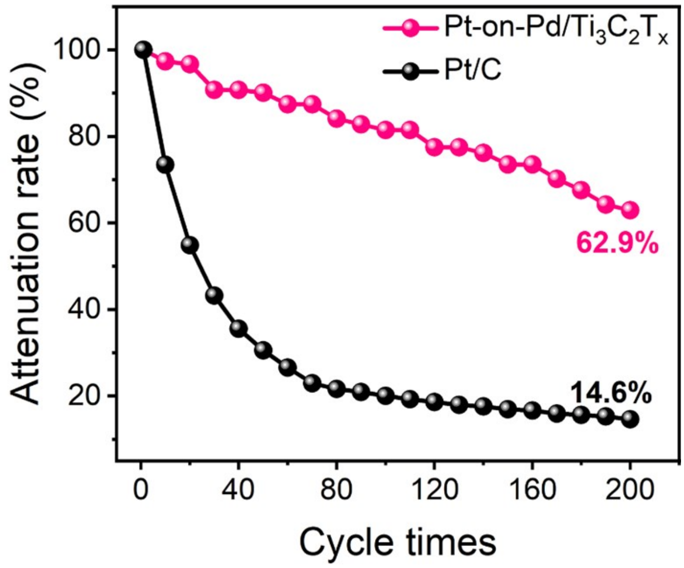

Fig. S12 The stability behaviors of Pt-on-Pd/$Ti_3C_2T_x$ and Pt/C catalysts toward methanol oxidation, revealing the better cycling stability of Pt-on-Pd/$Ti_3C_2T_x$ catalysts.

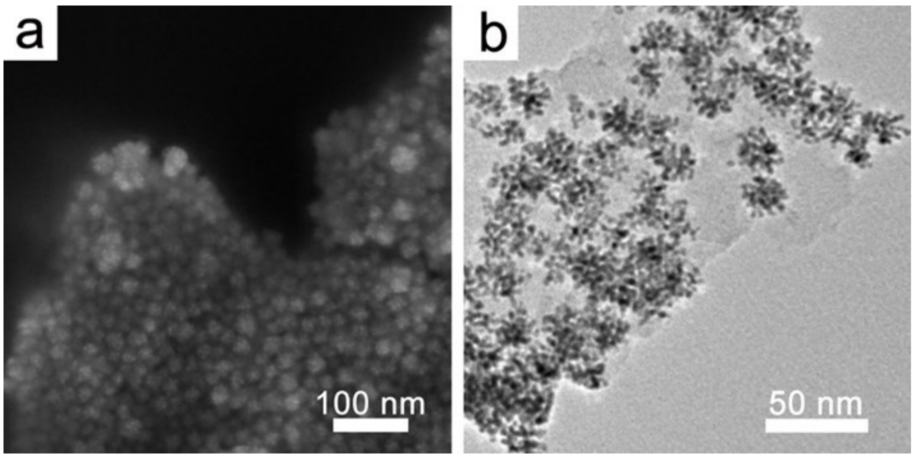

Fig. S13 Typical (A) SEM and (B) TEM images of the Pt-on-Pd/$Ti_3C_2T_x$ nanoarchitecture after the long-term chronoamperometric test.

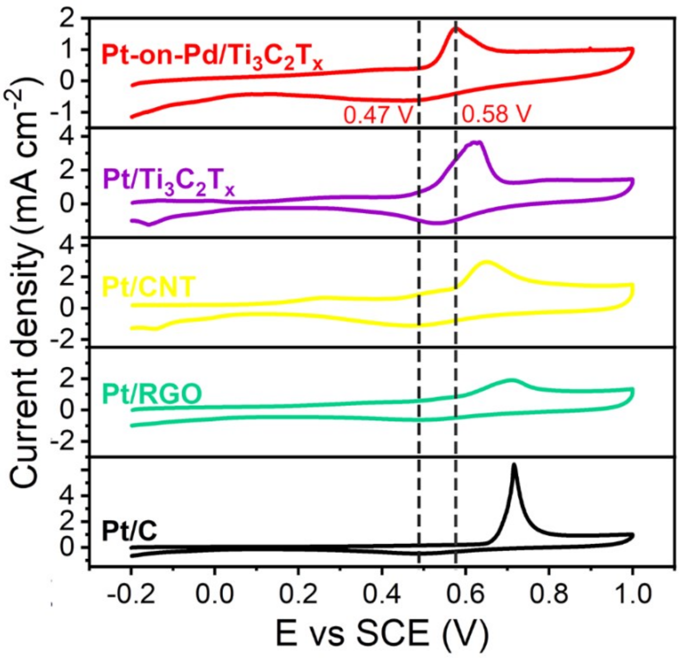

Fig. S14 CO stripping voltammograms for the Pt-on-Pd/$Ti_3C_2T_x$ samples Pt/$Ti_3C_2T_x$, Pt/CNT, Pt/RGO, and Pt/C catalysts tested in 0.5 M H_2SO_4 solution.

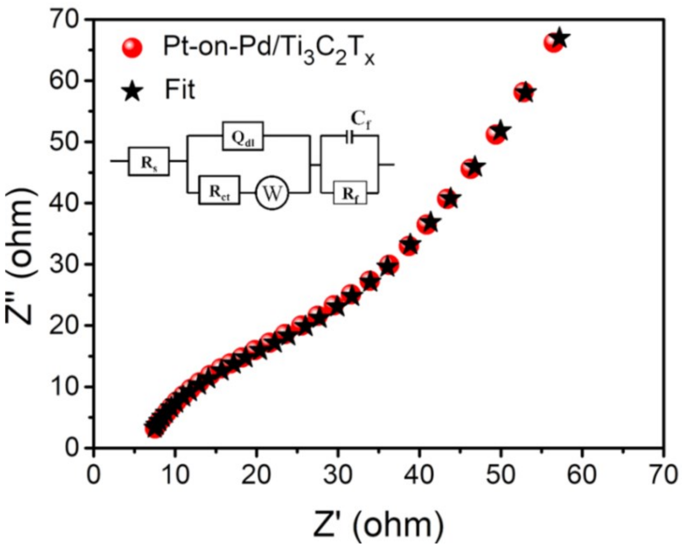

Fig. S15 AC impedance spectrum of the Pt-on-Pd/$Ti_3C_2T_x$ electrode and the corresponding fitting curve. The inset is the equivalent circuit: R_s and R_{ct} represent the resistances for electrolyte and catalyst, respectively, Q_{dl} is a constant phase element, W represents semiinfinite diffusion at the electrolyte/electrode interface, R_f and C_f are the resistance and capacitance for the Nafion-carbon film, respectively.

Table S1. Compiled study comparing ECSA and CV results for different catalysts.

Electrode	ECSA ($m^2 g^{-1}$)	Mass activity (mA mg^{-1})	Specific activity (mA cm^{-2})
Pt-on-Pd/$Ti_3C_2T_x$	157.3	1461.7	0.93
Pt-on-Pd/C	67.9	325.7	0.48
Pt/$Ti_3C_2T_x$	31.9	215.0	0.67
Pt/RGO	27.6	313.3	0.72
Pt/CNT	27.1	173.0	0.64
Pt/C	23.1	106.0	0.46

Table S2. Comparison of methanol oxidation behavior on the Pt-on-Pd/$Ti_3C_2T_x$ hybrids and various Pt-based electrocatalysts.

Catalyst	ECSA ($m^2 g^{-1}$)	Mass activity (mA mg^{-1})	Scan rate (mV s^{-1})	Electrolyte	Ref.
Pt-on-Pd/$Ti_3C_2T_x$	157.3	1461.7	50	0.5 M H_2SO_4+ 1 M CH_3OH	This work
AuPtCu nanowires	N.A.	~500.0	50	0.1 M $HClO_4$ + 1 M CH_3OH	S1
FePtPd nanowires	N.A.	488.7	50	0.1 M $HClO_4$ + 0.2 M CH_3OH	S2
PtPd/graphene	81.6	647.2	50	0.5 M H_2SO_4 + 1 M CH_3OH	S3
Pt/N-doped G	N.A.	~400.0	200	0.5 M H_2SO_4 +1MCH_3OH	S4
Pt/N-doped G nanoribbon	64.6	~390.0	20	1 M H_2SO_4 + 2 M CH_3OH	S5
Pt/imidazolium-salt ionic liquid/CNT	67.6	`410.0	50	0.5 M H_2SO_4 + 0.5 M H_3OH	S6
Pt/[BMIM]BF_4/CNT	N.A	155.0	50	0.5 M H_2SO_4 + 1 M CH_3OH	S7
Pt/mesoporous carbon	N.A.	~450	20	0.5 M H_2SO_4 + 1 M CH_3OH	S8
Pt/macroporous carbon	N.A.	81.6	50	0.5 M H_2SO_4 + 0.5 M CH_3OH	S9
Pt/3D MoS_2-G	62.3	~91.8	10	1 M H_2SO_4 + 2 M CH_3OH	S10

Reference

[S1] W. Hong, J. Wang, E. Wang, *Small* 2014, **10**, 3262.

[S2] S. Guo, S. Zhang, X. Sun, S. Sun, *J. Am. Chem. Soc.* 2011, **133**, 15354.

[S3] Guo, S.; Dong, S.; Wang, E., *Acs Nano* 2010**, 40**, 547.

[S4] B. Xiong, Y. Zhou, Y. Zhao, J. Wang, X. Chen, R. O'Hayre, Z. Shao, *Carbon* 2013, **52**, 181.

[S5] H. Huang, G. Ye, S. Yang, H. Fei, C. S. Tiwary, Y. Gong, R. Vajtai, J. M. Tour, X. Wang, P. M. Ajayan, *J. Mater. Chem. A* 2015, **3**, 19696.

[S6] S. Guo, S. Dong, E. Wang, *Adv. Mater.* 2010, **22**, 1269.

[S7] H. Chu, Y. Shen, L. Lin, X. Qin, G. Feng, Z. Lin, J. Wang, H. Liu, Y. Li, *Adv. Funct. Mater.* 2010, **20**, 3747.

[S8] H. Jiang, T. Zhao, C. Li, J. Ma, *Chem Commun* 2011, **47**, 8590.

[S9] X. Bo, L. Guo, *Electrochim. Acta* 2013, **90**, 283.

[S10] Z. Gao, M. Li, J. Wang, J. Zhu, X. Zhao, H. Huang, J. Zhang, Y. Wu, Y. Fu, X. Wang, *Carbon* 2018, **139**, 369.